ISSN: 2277-9655
Scientific Journal Impact Factor: 3.449
(ISRA), Impact Factor: 1.852

IJESRT

INTERNATIONAL JOURNAL OF ENGINEERING SCIENCES & RESEARCH TECHNOLOGY

Equilibrium and Kinetics of Glass Beads and Activated Carbon for Removal of Pb (II), Hg (II), and Cd (II) from Wastewater by Adsorption

Abbas Hamid Sulaymon, Shahlaa Esmail Ebrahim, Mohanad Jasim Mohammed Ridha
Environmental Engineering Department, College of Engineering, University of Baghdad
8856 Baghdad, Iraq
Environmental Engineering Department, College of Engineering, University of Baghdad
6382 Baghdad, Iraq
Environmental Engineering Department, College of Engineering, University of Baghdad
8752 Baghdad, Iraq
inas_abbas@yahoo.com

Abstract

The effect of partially replacing granular activated carbon (GAC) by glass beads (GB) in fixed bed for adsorption of Pb(II), Hg(II), and Cd(II) ions onto activated carbon were investigated. Experiments were carried out to study the effect of various GAC-GB weight ratio, adsorbate concentration, flow rate and bed depth on the performance of fixed bed. Isotherm experiments show that the results of Langmuir isotherm model is the best fit, the adsorption data R^2, 0.9816, 0.822, and 0.810 for Pb (II), Hg (II), and Cd (II) respectively. Optimum pH was found to be 4 for Pb(II), Hg(II) and 6 for Cd(II). While contact time was 360 min for each pollutant. Results suggest that replacing 5% by weight GAC by GB increasing the breakthrough time by 80% while, replacing 10% of GAC makes the adsorption inefficient compared with 0% GB. A general rate model (GRM) was formulated to describe the mass transfer kinetics in the fixed bed adsorber. The GRM includes external mass transfer and pore diffusion coefficient using nonlinear isotherms, provides a good description of the adsorption process.

Keywords: Adsorption, activated carbon, glass beads, heavy metals, general rate model, pore diffusion coefficient, mass transfer coefficient.

Introduction

The intensification of industrial activity during recent years is greatly contributing to the increase of heavy metals in the environment, mainly in the aquatic systems [1]. Wastewater contained with heavy metals is a serious environmental problem because they do not undergo biodegradation and are accumulated into the organism entering into the food chains [2]. Metals can be toxic to microbial population at sufficiently high concentrations. However, some metals are markedly more toxic even at very low levels. Among the toxic heavy metals, lead, mercury, and cadmium, ions ‘‘called the big three’’ are in the limelight due to their major impact on the environment; Lead and cadmium are potent neurotoxic metals [3]. The sources of human exposure to Cd (II) include atmospheric, terrestrial, and aquatic routes [4]. The most severe form of Cd (II) toxicity in humans is ‘‘itai-itai’’ [5]. Other health implications of Cd (II) in humans include kidney dysfunction, hepatic damage, and hypertension [6,7].

Lead is heavy metal poison which forms complexes with oxo-groups in enzymes to affect virtually all steps in the process of hemoglobin synthesis and prophyrin metabolism. Toxic levels of Pb (II) in man have been associated with encephalopathy seizures and mental retardation [1].

Mercury pollution results from metallurgical industries, chemical manufacturing, and metal finishing industries. Hg (II) in the liquid form is not dangerous and it is used in a number of industries. In the vapor form mercury becomes very poisonous. It attacks the lungs, kidneys, and the brain. The vapor crosses the blood–brain and blood stream [9].
Adsorption has been shown to be the most promising option for all these non-biodegradable heavy metals

ISSN: 2277-9655
Scientific Journal Impact Factor: 3.449
(ISRA), Impact Factor: 1.852

for the removal from aqueous streams, activated carbon being the most common adsorbent for this process due to its effectiveness and versatility. Although activated carbon, in granular or powdered form has a good capacity for the adsorption of heavy metals, it suffers from a number of disadvantages. Activated carbon is quite expensive and the higher the quality the greater the cost. Both chemical and thermal regeneration of spent carbon are expensive [10].

To design and operate a fixed bed adsorption process successfully, the column dynamics must be understood; that is the breakthrough curves under specific operating conditions must be predictable. Several rate models have been developed that take into account an external film transfer rate step, unsteady state transport in the solid phase and nonlinear equilibrium isotherm to predict adsorption rates in batch reactor and fixed bed [11]. Under a wide range of operating conditions, the key process parameters in adsorption such as isotherm constants and mass transfer coefficients are obtained by conducting batch studies of adsorption.

The liquid hold-up is an important characteristic of packing owing to its relation to the wetted area. There are two types of hold-up; static and dynamic (operating) hold-up. The static hold-up was measured as the weight of liquid retained when the column has drained to a constant weight; this was deducted from the total hold-up to obtain the operating hold-up. Investigators measured the hold-up for different aqueous solutions and they found that the static hold-up for carbon is greater than that for porcelain, which may be due to porosity of carbon material [12, 13].

The objective of this study is to investigate the effect of partially replacing activated carbon with glass beads for the removal of Pb (II), Hg (II), and Cd (II) by adsorption. This can be made more efficient and /or economical by increasing the adsorption surface area of the adsorbent through the reduction of dead zones between the particles in a fixed bed. To achieve this objective an experimental program was designed to use different GAC-GB weight ratios, Pb (II), Hg (II), and Cd (II) concentrations, flow rate and bed depth. The experimental results will compare with that obtained by theoretical formulation of the general rate model which includes axial dispersion, film mass transfer, pore diffusion resistance and nonlinear isotherm.

Theory

Fixed bed

Fixed bed dynamics are described by the convection-diffusion equations, coupled with source term due to adsorption and diffusion inside adsorbent particles. The solution of these equations will give rise to the prediction of the needed breakthrough curves [14,15].

The rate model considers the following; axial dispersion, external mass transfer, interparticle diffusion and nonlinear isotherm [16, 17].
The model equations are based on the hypothesis of an interparticle mass transfer controlled by diffusion into macropores (pore diffusion model), and this approach considers three phases; they are: the mobile phase in the space between particles, the stagnant film of mobile phase immobilized in the macropores and the stationary phase where adsorption occurs [18, 19].

The following basic assumptions are made in order to formulate the model, adsorption process is isothermal, the packing material is porous, spherical, particles of uniform size, the concentration gradient in the radial direction of the bed is negligible, local equilibrium exists for the component between the pore surface and the stagnant fluid phase in the pores, the film mass transfer mechanism can be used to describe the interfacial mass transfer between the bulk-fluid and particle phase, the dispersion coefficient is constant, and surface diffusion can be ignored.

Continuity equation of the mobile phase is:

$$-D_b \frac{\partial^2 C_b}{\partial Z^2} + \nu \frac{\partial C_b}{\partial Z} + \frac{\partial C_b}{\partial t} + \rho_p \frac{1-\varepsilon_b}{\varepsilon_b} \frac{\partial q}{\partial t} = 0 \qquad (1)$$

ISSN: 2277-9655
Scientific Journal Impact Factor: 3.449
(ISRA), Impact Factor: 1.852

Using C_p, the concentration in the stagnant mobile phase and writing the expression of the interfacial flux leads to [15]:

$$\rho_p \frac{\partial q}{\partial t} = \frac{3k_f}{R_p}\left(C_b - C_{p,R=R_p}\right) \tag{2}$$

Substituting Eq. (2) in Eq. (1) gives:

$$-D_b \frac{\partial^2 C_b}{\partial Z^2} + \nu \frac{\partial C_b}{\partial Z} + \frac{\partial C_b}{\partial t} + \frac{3k_f(1-\varepsilon_b)}{\varepsilon_b R_p}\left[C_b - C_{p,R=R_p}\right] = 0 \tag{3}$$

The particle phase continuity equation in spherical coordinates is:

$$(1-\varepsilon_p)\frac{\partial C_p^*}{\partial t} + \varepsilon_p \frac{\partial C_p}{\partial t} - \varepsilon_p D_p \left[\frac{1}{R^2}\frac{\partial}{\partial R}\left(R^2 \frac{\partial C_p}{\partial R}\right)\right] = 0 \tag{4}$$

The initial and boundary conditions can be represented by the following equations:

Initial condition (t = 0):

$$C_b = C_b(0, Z) = 0 \tag{5}$$

$$C_p = C_p(0, R, Z) = 0 \tag{6}$$

Boundary conditions:

Z = 0: $$\frac{\partial C_b}{\partial Z} = \frac{\nu}{D_b}\left(C_b - C_o\right) \tag{7}$$

Z=L: $$\frac{\partial C_b}{\partial Z} = 0 \tag{8}$$

R=0: $$\frac{\partial C_p}{\partial R} = 0 \tag{9}$$

R=R_p: $$\frac{\partial C_p}{\partial R} = \frac{k_f}{\varepsilon_p D_p}\left(C_b - C_{p,R=R_p}\right) \tag{10}$$

Defining the following dimensionless formula [19]:

$$c_b = \frac{C_b}{C_o} \quad , \quad c_p = \frac{C_p}{C_o} \quad , \quad c_p^* = \frac{C_p^*}{C_o} \quad , \quad r = \frac{R}{R_p} \quad , \quad z = \frac{Z}{L}$$

$$\tau = \frac{\nu t}{L} \quad , \quad Pe_L = \frac{\nu L}{D_b} \quad , \quad Bi = \frac{k_f R_p}{\varepsilon_p D_p} \quad , \quad \eta = \frac{\varepsilon_p D_p L}{R_p^2 \nu} \quad , \quad \zeta = \frac{3Bi\,\eta(1-\varepsilon_b)}{\varepsilon_b}$$

The model equations can be transformed into the following dimensionless equations:

$$-\frac{1}{Pe_L}\frac{\partial^2 c_b}{\partial z^2} + \frac{\partial c_b}{\partial z} + \frac{\partial c_b}{\partial \tau} + \zeta\left(c_b - c_{p,r=1}\right) = 0 \tag{11}$$

ISSN: 2277-9655
Scientific Journal Impact Factor: 3.449
(ISRA), Impact Factor: 1.852

$$\frac{\partial}{\partial \tau}\left[\left(1-\varepsilon_p\right)c_p^* + \varepsilon_p c_p\right] - \eta\left[\frac{1}{r^2}\frac{\partial}{\partial r}\left(r^2\frac{\partial c_p}{\partial r}\right)\right] = 0 \quad (12)$$

The concentration c_p* in Eq. (12) is the dimensionless concentration in the solid phase of the particles. It is directly linked to the isotherm, which is the extended Langmuir model:

$$C_p^* = \frac{q_m b \rho_p C_p}{1 + bC_p} \quad (13)$$

The initial conditions become:

($\tau = 0$):

$$c_b = c_b(0,z) = 0 \quad (14)$$

$$c_p = c_p(0,r,z) = 0 \quad (15)$$

And boundary conditions become;

z=0: $$\frac{\partial c_b}{\partial z} = Pe_L\left(c_b - 1\right) \quad (16)$$

z=L: $$\frac{\partial c_b}{\partial z} = 0 \quad (17)$$

r=0: $$\frac{\partial c_p}{\partial r} = 0 \quad (18)$$

r=1: $$\frac{\partial c_p}{\partial r} = Bi\left(c_b - c_{p,r=1}\right) \quad (19)$$

The concentration c_p* in dimensionless form:

$$c_p^* = \frac{\rho_p q_m b c_p}{1 + bC_o c_p} \quad (20)$$

Finite element method is used for discretization of the bulk-fluid phase partial differential equation and the orthogonal collocation method for the particle phase equation, an ordinary differential equation system is produced. The ordinary differential equation system with initial values can be readily solved using an ordinary differential equation solver such as the subroutine "ODE15S" of MATLAB which is a variable order solver based on the numerical differentiation formulas (NDFs). Optionally it uses the backward differentiation formulas (BDFs), which is also known as Gear's method.

Batch adsorber

The batch model is the following:

-Mass balance in the bulk-fluid phase

$$V_L\frac{dC_b}{dt} + \frac{3W_A}{\rho_p R_p}k_f\left(C_b - C_{p,r=R_p}\right) = 0 \quad (21)$$

Where V_L = volume of fluid in the batch adsorber, W_A = mass of activated carbon in the batch adsorber.

-Mass balance inside the particle

The solute diffusion inside a spherical particle is described by the following equation:

ISSN: 2277-9655
Scientific Journal Impact Factor: 3.449
(ISRA), Impact Factor: 1.852

$$\varepsilon_p \frac{\partial C_p}{\partial t} + \rho_p \frac{dq}{dt} = \varepsilon_p D_p \frac{1}{r^2} \frac{\partial}{\partial r}\left(r^2 \frac{\partial C_p}{\partial r} \right) \qquad (22)$$

The solute concentration in the pores is in local equilibrium with the concentration of solute adsorbed on the pore walls.

Initial and boundary conditions are:

$$t = 0 \quad , \quad C_b = C_o \quad , \quad C_p = 0$$

$$r = 0 \quad , \quad \frac{\partial C_p}{\partial r} = 0 \quad , \quad \frac{dq}{dr} = 0$$

$$r = R_p \quad , \quad \varepsilon_p D_p \frac{\partial C_p}{\partial r} = K_f (C_b - C_p)_{r=R_p}$$

For Langmuir isotherm model:

$$q = \frac{q_m b C_p}{1 + b C_p} \qquad (23)$$

The external mass transfer coefficient (k_f) for the solute adsorbed at certain particle size and optimum speed can be obtained by the analytical solution [20, 21].

$$k_f = -\frac{R_p \rho_p V_L}{3 W_A t} \ln\left(\frac{C_t}{C_o} \right) \qquad (24)$$

Where R_p and ρ_p the particle radius and density respectively and C_0 and C_t are the solute concentration at time zero and time t, respectively. Experimental concentration-time data are compared to predicted concentration-time profile for the above batch absorber model and the best statistical description used to determine the interparticle diffusion coefficient.

Experimental work

Materials

Adsorbate: A stock solution of lead, mercury and cadmium ions with a concentration of (1000 mg/l) were prepared by using Pb $(NO_3)_2$, $HgCl_2$ and Cd $(NO_3)_2$. The salts obtained from local market. Metal concentrations were determined by a flame atomic absorption spectrophotometer (type, Buck 210, USA). Adsorbent: The mesh size of the granular activated carbon (GAC) used in the experiment was 0.55 mm. The required sieve fraction was washed and dried in an oven that was maintained at 100°C to dry for 24 h, after which the GAC was kept in a desiccators.

Inert materials: Glass beads were supplied from the local markets.

Methods

For the determination of adsorption isotherms, 250 ml flasks filled with known concentration of solute and a known weight of activated carbon. The flasks placed on a shaker and agitate continuously for 6 h at 33±3°C. The concentration of solute in the solution determined using atomic absorption spectrophotometer. This experiment carried out for each adsorbate. The adsorbed amount is calculated by the following equation:

$$q_e = \frac{V (C_o - C)}{W} \qquad (25)$$

Where q_e is the internal concentration of solute per unit weight of activated carbon, V volume of the container, W weight of the activated carbon, and C_o and C are the initial and final solute concentrations.

The pore diffusion coefficients (D_p) and the external mass transfer coefficients for each solute were obtained by using a stirred batch contactor. In this method a known amount of adsorbent (GAC with particle size of 0.55 mm) is mixed with a constant volume of solute solution. A cylindrical cell was used with a capacity of $2\times10^{-3}m^3$. A 3-bladed stainless steel axial flow impeller was fixed at the center of the cylindrical cell (Type WiseStir, Korea). The cell was filled with 1.0 L of known concentration solution of each solute and the agitation started before adding the

ISSN: 2277-9655
Scientific Journal Impact Factor: 3.449
(ISRA), Impact Factor: 1.852

GAC particles. At time zero, the accurate mass of GAC was added. Samples were taken every (15 min) during the experiment. The optimum agitation speed was obtained by repeating the experiments for each solute with variable speeds (400,600,800,900 and 1000 rpm). The batch experiments were achieved at constant temperature (30ºC).The necessary dosage of activated carbon to reach equilibrium related concentration of C /Co equal 0.05, were calculated by using Eq. (25).

The effect of pH and optimum contact time on Pb (II), Hg (II) and Cd (II) ions adsorption onto GAC was studied; 0.1 g of GAC was mixed with 100 ml of single metal ion solution concentration of 50 mg/l of Pb (II), Hg (II) and Cd (II) ions. These were maintained at different pH values ranging from 3 to 8 by using 0.1 M NaOH or HNO_3 solution, The pH values were measured using pH meter (Type Lovibond) as. The flasks placed on a shaker at agitation speed 200 rpm for a period of 360 min and 30°C.

The fixed bed experiments carried out in a column of 50 mm (I.D) and 50 cm in height. The granular activated carbon confined in the column by fine stainless steel screen at the bottom and glass packing at the top of the bed to ensure a uniform distribution of influent through the carbon bed. The influent solution introduced to the column through a perforated plate fixed at the top of the column. Feed solution prepared in a vessel supplied with immersed heater with a thermocouple to adjust the temperature of the solution at 30ºC.

Results and discussion

Batch adsorber

pH and contact time,

Figure 1 represents the relationship between pH values for the three adsorbates with the uptake (q_e). Optimum pH for Pb (II) and Hg (II) ions were 4 while for Cd (II) ions was 6. **Figure 2** indicates the effect of contact time where the uptakes of the three adsorbates increase at the beginning; this is probably due to a larger surface area of the GAC being available. As the surface adsorption sites become exhausted, the uptake rate is controlled by the rate at which the adsorbate is transported from the exterior to the interior sites of the adsorbent particles. The increase in the contact time increases the Pb (II), Hg (II), and Cd (II) adsorption and it remains constant after reaching equilibrium. The maximum uptakes of Pb (II), Hg (II), and Cd (II) were attained after about 360 min of shaking time. Therefore, 360 min was selected as optimum shaking time.

Adsorption isotherm results

The adsorption data were fitted five models. The correlation coefficients (R^2) are shown in **Table 1**. This table indicates that the Langmuir model provides the best fit as judged by its R^2. Therefore Langmuir model was selected to be used in the fixed bed. **Figure 3** represents the adsorption isotherm for Pb(II), Hg(II) and Cd(II) onto GAC. Results can be compared in term of adsorption capacity: Pb(II)>Hg(II)>Cd(II). Due to the electronegativities of Pb(II) are higher than Hg(II) and Cd(II) 2.33, 2.0 and 1.69, respectively, and low solubility in water, 52, 7.4 ,136 g/100ml for Pb(II), Hg(II), and Cd(II), therefore, Pb(II) has higher strength of covalent binding than the lower affinity metals ions Hg(II) and Cd(II). As the electronegativity of the atom increases, its ionic forms seem to be more easily adsorbed onto the adsorbent [22].

Pore diffusion coefficient in batch adsorber

The doses of GAC used for adsorption of Pb(II), Hg (II), and Cd (II) were calculated for final equilibrium C_e/C_o=0.05. The Langmuir model constants were used with the mass balance in 1 L of solution. The initial concentration was 50 mg/L with the doses of GAC of 10.298, 12.55, and 70.78 gm for the Pb (II), Hg (II), and Cd (II) respectively. The agitation speeds (400, 600, 800, 900, and 1000,) were used for Pb (II), Hg (II), and Cd (II) **Figure 4 (a,b,c)**. The optimum agitation speed to achieve C_e/C_o=0.05 was 800 rpm for each solute. It is clear that, if the speed is above 800 rpm, C_e/C_o is less than 0.05; this is due to pulverization of activated carbon at high speed agitation.

The external mass transfer coefficient (k_f) was calculated from the concentration decay curve of optimum speed, using **Eq. (24).** For estimation of k_f, samples were taken at 3, 6 and 9 min. The average mass transfer coefficient for Pb (II), Hg (II), and Cd (II) adsorption are 8.35036×10^{-6}, 3.50997×10^{-6}, and 2.64044×10^{-6} m/s respectively.

Pore diffusion coefficient was obtained from the numerical solution of **Eqs. (21)** and **(22)** with appropriate initial and boundary conditions that describe the film and interparticle transport mechanisms, using the external mass transfer coefficient k_f.

The pore diffusion coefficient was derived from the typical concentration decay curve by an iterative search technique predicted on the minimization of the difference between experimental and predicted data from pore diffusion model. It is clear from **Figure 5**, that there were a good matching between experimental

ISSN: 2277-9655
Scientific Journal Impact Factor: 3.449
(ISRA), Impact Factor: 1.852

and predicted data by using pore diffusion model for Pb(II), Hg(II), and Cd(II). The pore diffusion coefficients for the solutes were found to be; 6.32×10^{-10}, 4.68×10^{-10}, and 1.73×10^{-10} m^2/s respectively. The external mass transfer coefficients in packed bed were evaluated by using the correlation of Wilson and Geankoplis [23].

$$Sh = \frac{1.09}{\varepsilon_b} S_c^{1/3} R_e^{1/3} \qquad 0.0015 < \mathrm{Re} < 55 \qquad (26)$$

Where:

$$\mathrm{Re} = \frac{2R_p \rho_w \nu}{\mu_w} \qquad Sh = \frac{k_f 2R_p}{D_m} \qquad Sc = \frac{\mu_w}{\rho_w D_m} \qquad \nu = \frac{Q}{A\varepsilon_b}$$

The molecular diffusion coefficient D_m of Pb (II), Hg (II), and Cd (II) in aqueous solution are 4.98×10^{-8}, 3.15×10^{-9}, and 4.2×10^{-8} m^2/s respectively. These values are substituted in Eq. (26) to evaluate K_f at different interstitial velocities.

The axial dispersion coefficient D_b is estimated from Chung and Wen correlation [24]

$$\frac{\nu 2\gamma}{D_b} = \frac{L}{2\varepsilon_b R_P}\left(0.2 + 0.011\,\mathrm{Re}^{0.48}\right)$$

Packed bed adsorber

Effect of different activated carbon-glass beads weight ratios

The effect of different activated carbon-glass beads weight ratios were investigated for Pb (II), Hg (II), and Cd (II) adsorption in term of C/C_o versus time. The experimental breakthrough curve for Pb (II) adsorption is presented in **Figure 6,** while **Figure 7 (a, b, c)** represent the experimental and theoretical breakthrough curves for each activated carbon-glass beads ratio, constant initial concentration of Pb (II), flow rate, bed depth, and pH.

Figure 8 shows breakthrough curves for Pb (II) adsorption using 0%, 5%, and 7% of GB, it can be seen from this curve that the breakpoint for 5% is nearly identical with the breakpoint of 0%. Increasing the glass beads ratios to 7% make the adsorption process not efficient compared with 0% glass beads ratio. At 0%, 5%, and 7% glass beads weight ratios the traces of Pb (II) values appear in the effluent of the bed are 0.0187, 0.00404, and 0.0367 after 3 min respectively.

Figure 9 represents the experimental and theoretical breakthrough curves for different activated carbon-glass beads weight ratios at constant initial concentration, constant flow rate, bed depth, and pH for Hg (II). It can be seen from this figure that the breakpoint for 5% glass beads bed ratio took longer time to appear than 7% and 0%. Where at 0% glass beads weight ratio the traces of Hg (II) appear in the effluent of the bed after 1 min with C/Co value equal to 0.1334 while, at 5% the traces in the effluent appear after 3 min with C/Co value equal to 0.0013 while at 7% the traces in the effluent also appear after 3 min with C/Co value equal to 0.0062. The difference in the Hg (II) adsorption behavior than Pb (II) may be attributed to the difference in the molecular diffusion.

Figure 10 shows experimental breakthrough curves when 0%, 5%, and 7% of glass beads for Cd (II), while **Figures 11(a, b, c)** represent the experimental and theoretical breakthrough curves for each activated carbon-glass beads ratio. It can be seen from **Figure 12** that the breakpoint for 5% is nearly identical with the breakpoint at 0%. Increasing the glass beads ratios to 7% make the adsorption process not efficient compared with 0%. At 0%, 5%, and 7% glass beads weight ratios the traces of Cd (II) values appear in the effluent of the bed are 0.2311, 0.1001, and 0.3167 after 1 min respectively. It can be seen from the above that replacing 5% by weight GAC by glass beads for Pb (II), Hg (II) and Cd (II) adsorption systems give a better behavior than pure GAC bed, this may be attributed to the nature of the activated carbon particles where it is entirely different from the glass beads regarding the roughness of the surface and the porosity of the material. The glass beads have more or less smooth surface, while the activated carbon particles have nearly rough surface.

ISSN: 2277-9655
Scientific Journal Impact Factor: 3.449
(ISRA), Impact Factor: 1.852

From the above and from the principle of liquid hold-up, it can be concluded that the static liquid hold-up is as follows:

Static hold-up for activated carbon-activated carbon particles > activated carbon-glass beads > glass-glass beads,

This leads to the losses in surface area for adsorption as follows:-

Area losses in activated carbon-activated carbon particles > activated carbon-glass beads,

The dynamic liquid hold-up will have the same behavior as mentioned above; this is related to the differences in the nature of activated carbon and the glass beads. Due to the roughness of the activated carbon surfaces, the operating liquid film thickness will be higher than that for the glass beads for a given particle diameter, flow rate, pollutant concentration and temperature. Therefore the phenomena will lead to high resident time for the liquid on the activated carbon particles compared with glass particles, and consequently increases the breakthrough time for the adsorption process. The bed porosities measured for different activated carbon-glass beads weight ratios and they were 0.4, o.43, and 0.45 for 0%, 5%, and 7% respectively. The increase in the bead porosities agree with mentioned above. Therefore, it is very important to find the optimum weight ratio of glass particles to activated carbon particles. Knowing that the matching between the two mechanisms; static hold-up and operating hold-up will save weight of activated carbon and minimize the losses in surface area for adsorption. These results agree with [13, 25].

Effect of influent concentration

The effect of varying Pb (II), Hg (II), and Cd (II) initial concentrations was investigated. The experimental and predicted breakthrough curves are presented in **Figures 11(a, b, c)** in term of C/C_o versus time. Constant concentrations, flow rate, pH, and bed depth with 5% glass beads ratio. It is clear from the breakthrough curves that an increase in the initial concentration for each solute makes the breakthrough curve much steeper, this is based on increasing driving force for mass transfer with increasing concentration of each adsorbate in solution. The same conclusion was obtained [26, 27].A high solute concentration may saturate the activated carbon more quickly, thereby decreasing the breakthrough time. The breakpoint was inversely related to the initial concentration. This may be also explained by the fact that since the rate of diffusion is controlled by the concentration gradient, it takes longer time to reach saturation for the case of low initial concentration [28, 29].

Effect of flow rate

The effect of varying the volumetric flow rate was investigated; the experimental and predicted breakthrough curves are presented in **Figure 12 (a, b, c)** in term of C/C_o versus time. The breakthrough curves were obtained for different adsorbate at constant initial concentration, bed depth 5% .glass beads ratio, and pH. Increasing the flow rate may be expected to make reduction of the surface liquid film. Therefore, this will decrease the resistance to mass transfer and increase the mass transfer rate. Also, because the reduction in the surface liquid film is due to the disturbance created when the flow of the feed increased resulting of easy passage of the adsorbate molecules through the particles and entering easily to the pores. This will decrease the contact time between adsorbate and activated carbon at high flow rate. These results agree with that obtained [27, 30]. The uptake of each solute by activated carbon appears to be controlled by particle diffusion. The same phenomena have been observed of activated carbon used for removing pollutants [31, 32].

Effect of bed depth

The effect of bed depth was investigated for Pb (II), Hg (II), and Cd (II) adsorption onto activated carbon, the experimental and predicted breakthrough curves are presented in **Figure 13(a, b, c)**. The breakthrough curves obtained for different bed depths with 5% glass beads bed ratio at constant flow rate, initial concentration, and pH for each adsorbate solution. Hence, the internal and external resistances are confirmed to be the main parameters that control the adsorption kinetics with the increase of bed depth. It is clear that increasing the bed depth increases the breakthrough time and the residence time of each adsorbate in the column. These results also agree with results obtained [31, 32].

Conclusions

The adsorption process can be made more efficient and/or economical by increasing breakthrough time via adding an inert material (glass beads) to the activated carbon bed in different weight ratios. The equilibrium isotherm data were correlated with five models for Pb (II), Hg (II), and Cd (II) adsorption, Langmuir model gave the best fit for the experimental data for each adsorbate. The batch experiments were helpful in estimating the isotherm

ISSN: 2277-9655
Scientific Journal Impact Factor: 3.449
(ISRA), Impact Factor: 1.852

model constants, external mass transfer coefficient, and interparticle pore diffusion coefficient. There was a good matching between experimental and predicted data in batch experiment by using pore diffusion method. Hence the transfer of each adsorbate within the activated carbon is controlled by pore diffusion. A general rate model which includes axial dispersion, film mass transfer, pore diffusion resistance and non-linear isotherms provides a good description of the adsorption process. An increase in the initial concentration of each adsorbate makes the breakthrough curves much steeper, which would be anticipated with the basis of increases driving force for mass transfer with the increase of each adsorbate concentration. The increase in the bed depth of activated carbon will increase the breakthrough time and the residence time of the each adsorbate solution in the column. While increasing the solute flow rate decreases the breakthrough time due to the decrease in the contact time between the adsorbate and the adsorbent along the adsorption bed.

Acknowledgment

We would like to express our sincere thanks and deep gratitude to the Arab Science and Technology Foundation (ASTF) for supporting this work financially.

Symbols

A_R	Reddlich-Peterson model parameter
B	Langmuir constant, L/mg
B_i	$\left(\frac{k_f R_p}{\varepsilon_p D_p}\right)$
B_R	Reddlich-Peterson model parameter
C	Concentration in fluid, kg/m^3
C_o	Initial concentration, kg/m^3
C_e	concentration of solute at equilibrium, kg/m^3
D_b	Axial dispersion coefficient, m^2/s
D_m	Molecular diffusion coefficient, m^2/s
D_p	Pore diffusion coefficient, m^2/s
d_p	Particle diameter, m
F_{RP}	Radke-Prausnitz model parameter
K	Freundlich empirical constant
k_f	Fluid to particle mass transfer coefficient, m/s
K_{RP}	Radke-Prausnitz model parameter
L	Length of bed, m
m_R	Reddlich-Peterson model parameter
N_{RP}	Radke-Prausnitz model parameter
n	Freundlich empirical constant
Pe	$\left(\frac{vL}{D_b}\right)$
Q	Fluid flow rate, m^3/s
q_e	The amount of adsorbate per unit weight of carbon at equilibrium (mg/mg)
q_m	Adsorption equilibrium constant defined by Langmuir equation, mg/gm
R_e	$\left(\frac{\rho_w v d_p}{\mu_w}\right)$
R_p	Radius of particle, m

ISSN: 2277-9655
Scientific Journal Impact Factor: 3.449
(ISRA), Impact Factor: 1.852

S_c	$\left(\frac{\mu_w}{\rho_w D_m}\right)$
Sh	$\left(\frac{k_f d_p}{D_m}\right)$
T	Time, s
V	$\left(\frac{Q}{A\varepsilon_b}\right)$, m/s
v_s	$\left(\frac{Q}{A}\right)$, m/s
V_L	Volume of solution, m^3
W_A	Mass of adsorbent, kg
Z	Axial distance, m
ε_b	Bed porosity
ε_p	Porosity of adsorbent
μ_w	Viscosity of water
ρ_w	Density of water, kg/m^3
ρ_p	Bulk density of adsorbent, kg/m^3

References

1. Sulaymon A., Ebrahim, S., and Ridha M "Equilibrium, kinetic, and thermodynamic biosorption of Pb(II), Cr(III), and Cd(II) ions by dead anaerobic biomass from synthetic wastewater, Environmental Science and Pollution Research .Vol.20, No.1, pp 175-87 ,2013a
2. Sulaymon A., Ebrahim, S., and Ridha M, "Competitive biosorption of Pb(II), Cr(III), and Cd(II) from synthetic wastewater onto heterogeneous anaerobic biomass in single, binary, and ternary batch systems" Desalination and Water Treatment, doi:10.1080/19443994.2013.813008, pp. 1-10, 2013.
3. Puranik, P.R. and Paknikar, K.M. , Biosorption of lead and zinc from solution using streptoverticillium waste biomass,J. Biotechnol., 55 (1997) 113–124.
4. Wolnik, K.A., Frick, F.L., Caper, S.G., Meyer, M.W. and Satzergar, R.D., Cadmium lead and eleven other elements in carrots field corn, onion, rice, spinach and tomatoes, J. Agric. Food Chem., 33(1985) 807–811.
5. Yasuda, M., Miwa, A. and Kitagawa, M., Morphometric studies of renal lesions in '' Itai-itai'' disease: chronic cadmium nephropathy, Nephron, 69 (1995) 14–19.
6. Klaassen, C.D., Hardmen, J.G., Limbird, L.E. and Gilman, A.G., the Pharmacological Basis of Therapeutics, McGraw Hill, New York, (2001).
7. Vahter, M., Berghund, M., Nermell, B. and Akesson, A., Bioavailability of cadmium from shell fish and mixed diet in women, Toxicol. Appl. Pharmacol., 136 (1996) 332–334.
8. Ademorati, C.M.A., Environmental Chemistry and Toxicology. Pollution by Heavy metals. Fludex press Ibadan (1996) 171–172.
9. Igwe, J.C. and Abia, A.A., A bioseparation process for removing heavy metals from wastewater using biosorbents, Afric. J. Biotechnol. 5 (12) (2006) 1167–1179.
10. Fu, Y. and Viraraghavan, T.F., Decolourization of wastewaters: a review, Bioresour. Technol., 79 (2001) 251–262.
11. Hsu, Y.C., Chiang, C.C. and Yu, M.F., Modeling and simulation for packed bed adsorption, Sep. Sci. Technol., 32 (1997) 2513.

ISSN: 2277-9655
Scientific Journal Impact Factor: 3.449
(ISRA), Impact Factor: 1.852

12. Crittenden, J.C. and Weber, W.J., Predictive model for design of fixed bed adsorbers: parameter estimation and model development. J. Env. Eng. Div., ASCE, 104 (1978) 185.
13. Sulaymon, A.H., and Ebrahim, Sh. E., , Saving amberlite XAD4 by using inert material in adsorption process, Desalination and Water Treatment, 20 (2010) 234–242.
14. Crittenden, J. C., Berrigan, J. K., , Hand, D. W. and Lykins, B. Design of rapid small-scale adsorption tests for a constant diffusivity. J. WPCF, 58(1986) 4, 312-319.
15. Gu, T. Mathematical modelling and scale-up of liquid chromatography. Springer, Berlin, (1995).
16. Guiochon, G., Shirazi, S. G. and Katti, A. Fundamentals of preparative and nonlinear chromatography. Academic Press, Boston, MA. (1994).
17. Ruthven, D. M., Principles of adsorption and adsorption processes. John Wiley and Sons, Inc., (1984).
18. Ganetson, G. and Barker, P. E., Preparative and production scale chromatography. Marcel Dekker, New York, (1993)
19. Eggers, R., Simulation of frontal adsorption. HIWI report by Hamburg-Hamburg University, (2000).
20. Alexander, P. M. and Zayas, I. Particle size and shape effects on adsorption rate parameters, J. Environmental Engineering, 115 (1989) 1, Feb., 41-55.
21. Liu, B., Yang, Y. and Ren, Q. Parallel pore and surface diffusion of levulinic acid in basic polymeric adsorbents, Journal of Chromatography A.,(2006), 1132, 190-200.
22. Chong, K., H., and Volesky, B., "Metal biosorption equilibria in a ternary system" Biotechnology and Bioengineering, (1995),49(6), 629-638.
23. Lucas, S. and Cocero, M. J., "Adsorption isotherms for ethylacetate and furfural on activated carbon from supercritical carbon dioxide" Fluid Phase Equilibria, (2004), 219, pp 171-179.
24. Gupta, A., Nanoti, O. and Goswami, A.N., The removal of furfu-ral from water by adsorption with polymeric resin. Separ. Sci. Technol., 36(13) (2001) 2835–2844.
25. Sulaymon, A. H., Mahdi, T., and Ebrahim, Sh. E., "Saving activated carbon by using inert materials in adsorption process" J.Int. Environmental Application & Science, Vol. 7(1): (2012): 101-113.
26. Lin, S. H. and Wang, C. S., "Treatment of high-strength phenolic wastewater by a new two-step method", Journal of Hazardous Materials, B90, (2002), pp 205-216.
27. Wa'adalla, K., "Removal of multi-pollutants from wastewater by adsorption method", Ph. D. Thesis, University of Baghdad, (2006).
28. Ivars, N., "Analysis of some adsorption experiments with activated carbon", Chem. Eng. Sci., (1976), 31, pp 1029-1035.
29. Malkoc, E. and Nuhoglu, Y., "Fixed bed studies for the sorption of chromium (VI) onto tea factory waste", Chemical Engineering Science, V.61, (2006), pp 4363-4372.
30. Babu, B.V. and Gupta, S., "Modelling and simulation for dynamics of packed bed adsorption", Chem. Conf., Mumbai, (2004).
31. Gupta, A., Nanoti, O. and Goswami, A.N., The removal of furfural from water by adsorption with polymeric resin. Separ. Sci. Technol., 36(13) (2001) 2835–2844.
32. Walker, G. M., Weatherley, L. R., "Fixed bed adsorption of acid dyes onto activated carbon", Environmental Pollution, V.99, (1998), 133-136.

ISSN: 2277-9655
Scientific Journal Impact Factor: 3.449
(ISRA), Impact Factor: 1.852

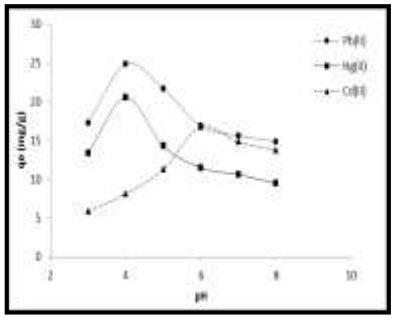

Fig.1 Effect of pH on the uptake of Pb(II), Hg(II) and Cd(II) ions onto GAC, C_{GAC} = 1 g/L, $C_{0(Pb,\ Cr\ and\ Cd)}$ = 50 mg/L, contact time = 6 h and agitation speed= 200 rpm.

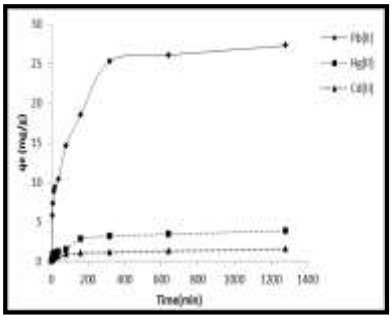

Fig. 2 Effect of contact time on the uptake of Pb(II), Hg(II) and Cd(II) ions onto GAC, C_{GAC} = 1 g/L,$C_{0(Pb,\ Hg\ and\ Cd)}$ = 50 mg/L, and agitation speed= 200 rpm

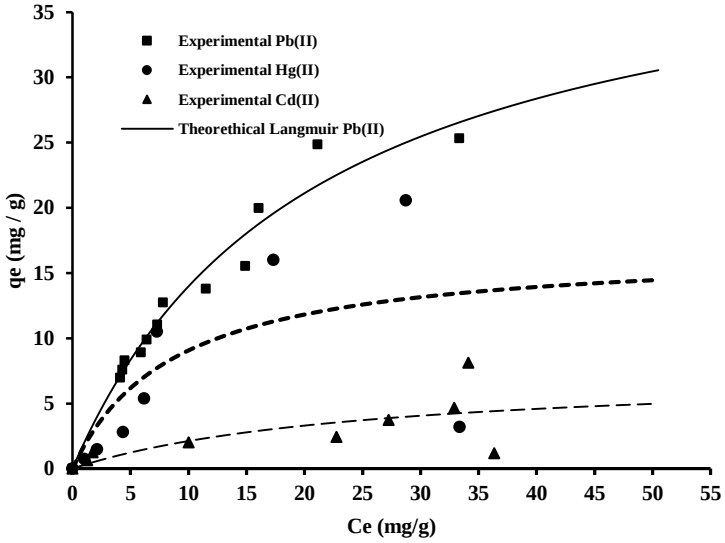

Fig. 3 Adsorption isotherm for Pb(II), Hg(II) and Cd(II) onto GAC

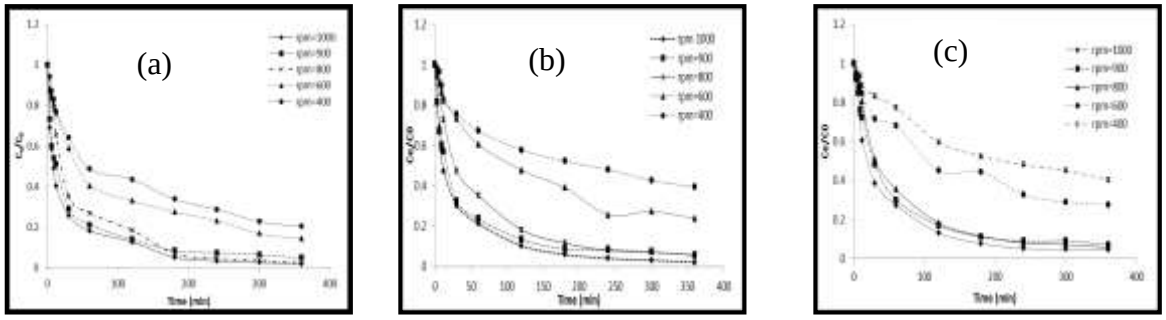

Fig. 4 Concentration-time decay curves for (a) Pb (II), (b) Hg(II) and (c) Cd (II) adsorption onto onto GAC at different agitation speed

ISSN: 2277-9655
Scientific Journal Impact Factor: 3.449
(ISRA), Impact Factor: 1.852

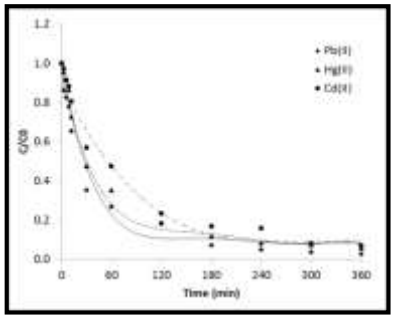

Fig.5 Comparison of the measured concentration-time data with that predicted (dashed lines) by pore diffusion model in batch adsorber for Pb (II), Hg (II), and Cd (II) systems

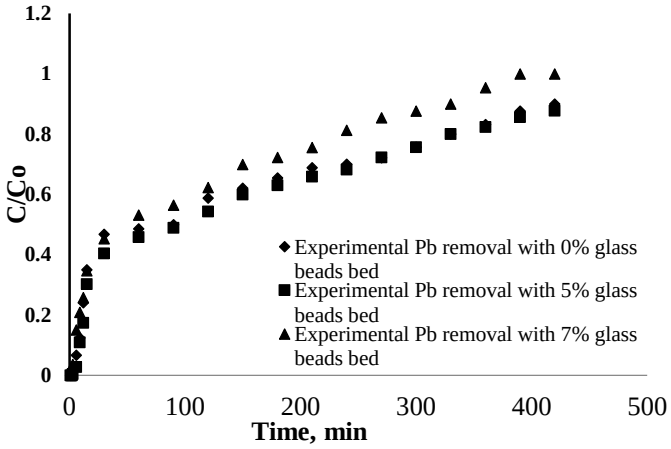

Fig.6 Experimental breakthrough curves for Pb (II) adsorption onto activated carbon at different glass beads ratios with: Q=2.78×10-6m^3/s, Co=50ppm, L=0.1 m, and pH=4

ISSN: 2277-9655
Scientific Journal Impact Factor: 3.449
(ISRA), Impact Factor: 1.852

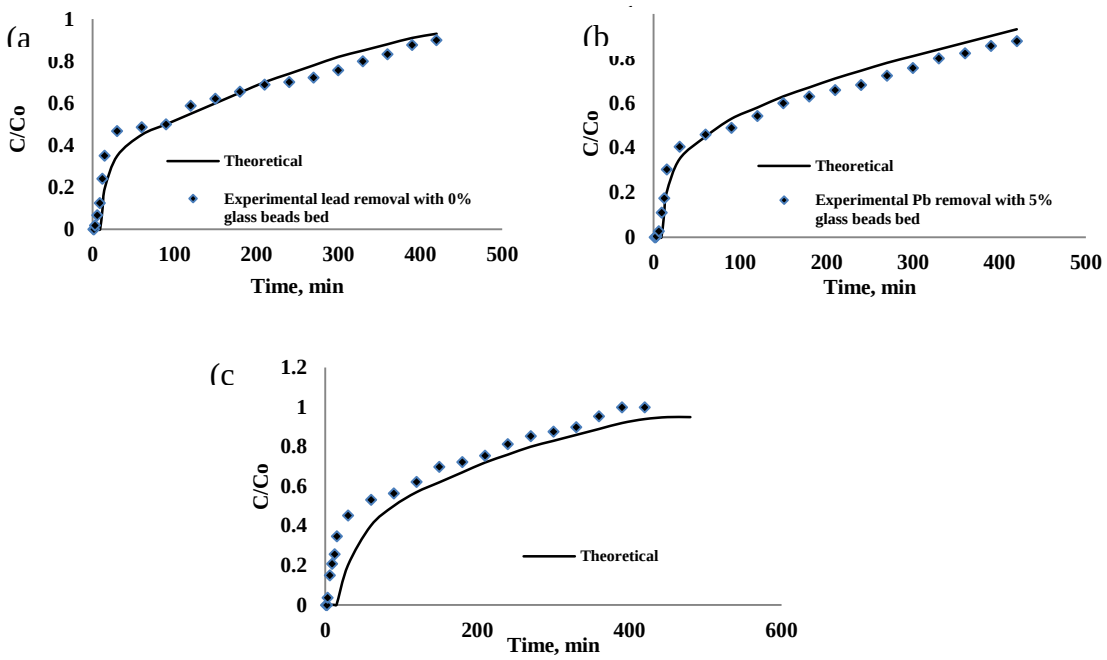

Fig. 7 Experimental and theoretical breakthrough curves of Pb(II) adsorption onto activated carbon at (a) 0% glass beads bed ration (b) 5% glass beads bed ratio (c) 7% glass beads bed ration with Q=2.78×10-6 m3/s, Co=50ppm, L=0.1 m, and pH=4

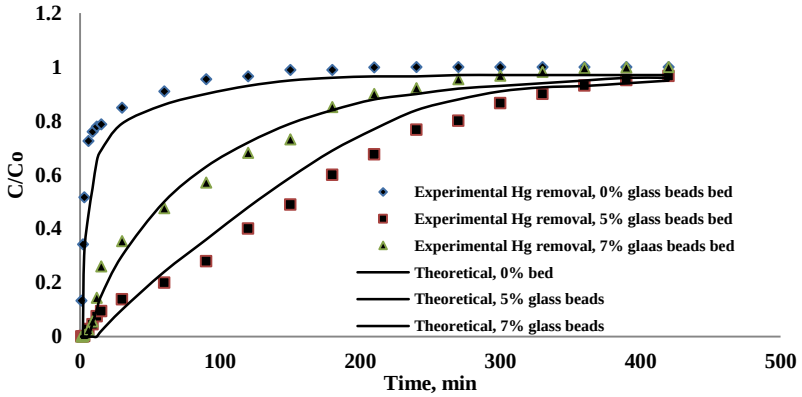

Fig. 8 Experimental and Theoretical breakthrough curves for Hg (II) adsorption onto activated carbon for different glass beads ratios with: Q=2.78×10-6m3/s, Co=50ppm, L=0.1 m, and pH=4

ISSN: 2277-9655
Scientific Journal Impact Factor: 3.449
(ISRA), Impact Factor: 1.852

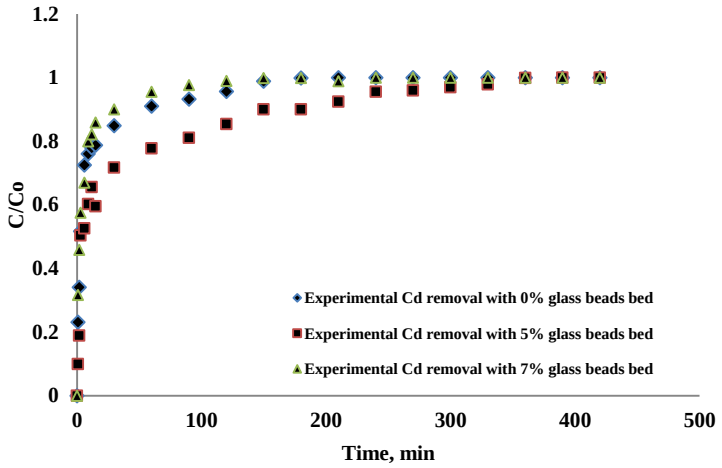

Fig. 9 Experimental breakthrough curves for Cd (II) adsorption onto activated carbon at different glass beads ratios with: Q=2.78×10-6m3/s, Co=50ppm, L=0.1 m, and pH=6

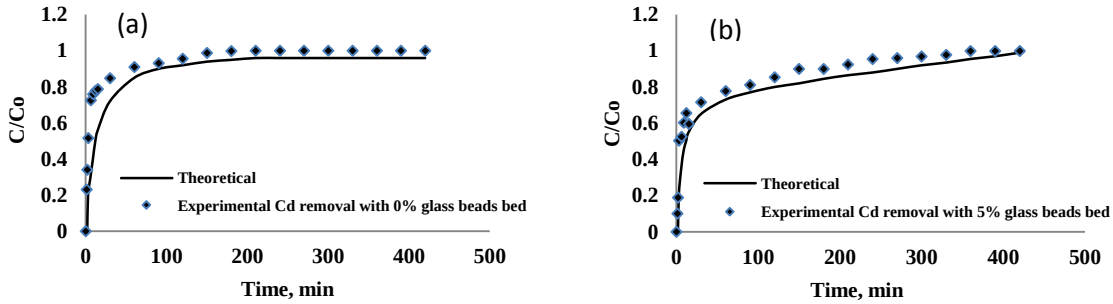

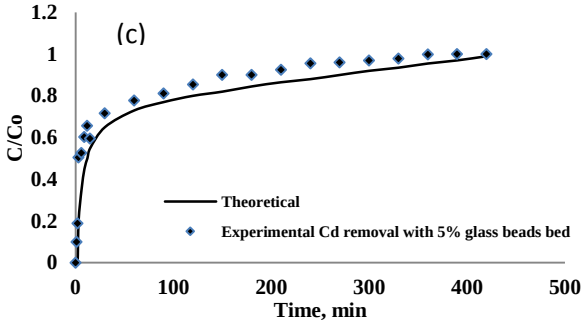

Fig. 10 Experimental and Theoretical breakthrough curves for Cd (II) adsorption onto activated carbon at (a) 0% glass beads bed ratio (b) 5% glass beads bed ratio (c) 7% glass beads bed ration with: Q=2.78×10-6 m3/s, Co=50ppm, L=0.1 m, and pH=6

ISSN: 2277-9655
Scientific Journal Impact Factor: 3.449
(ISRA), Impact Factor: 1.852

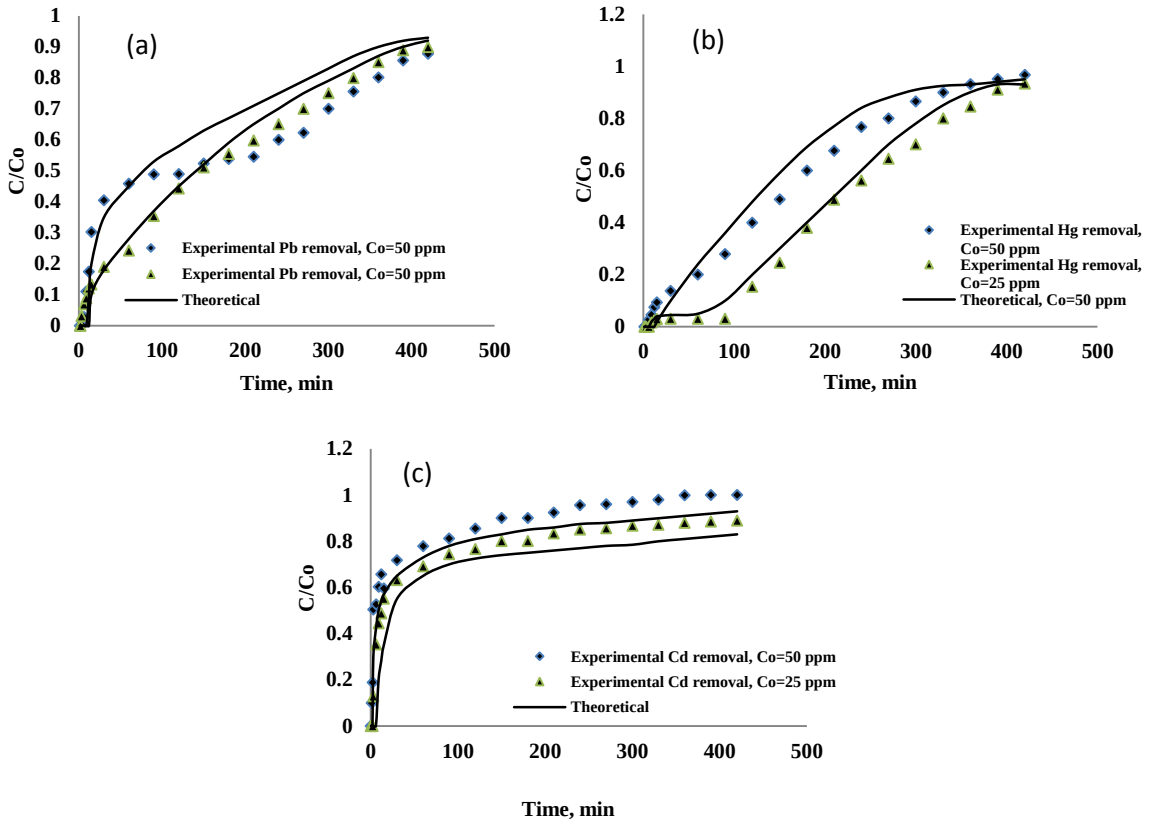

Fig. 11 Experimental and theoretical breakthrough curves for Pb (II), Hg (II) and Cd adsorption onto activated carbon at different initial concentration, Q=2.78×10-6m3/s, L=0.1 m (with 5% glass beads bed) and pH=4 for Pb(II) and Hg(II), pH=6 for Cd(II)

ISSN: 2277-9655
Scientific Journal Impact Factor: 3.449
(ISRA), Impact Factor: 1.852

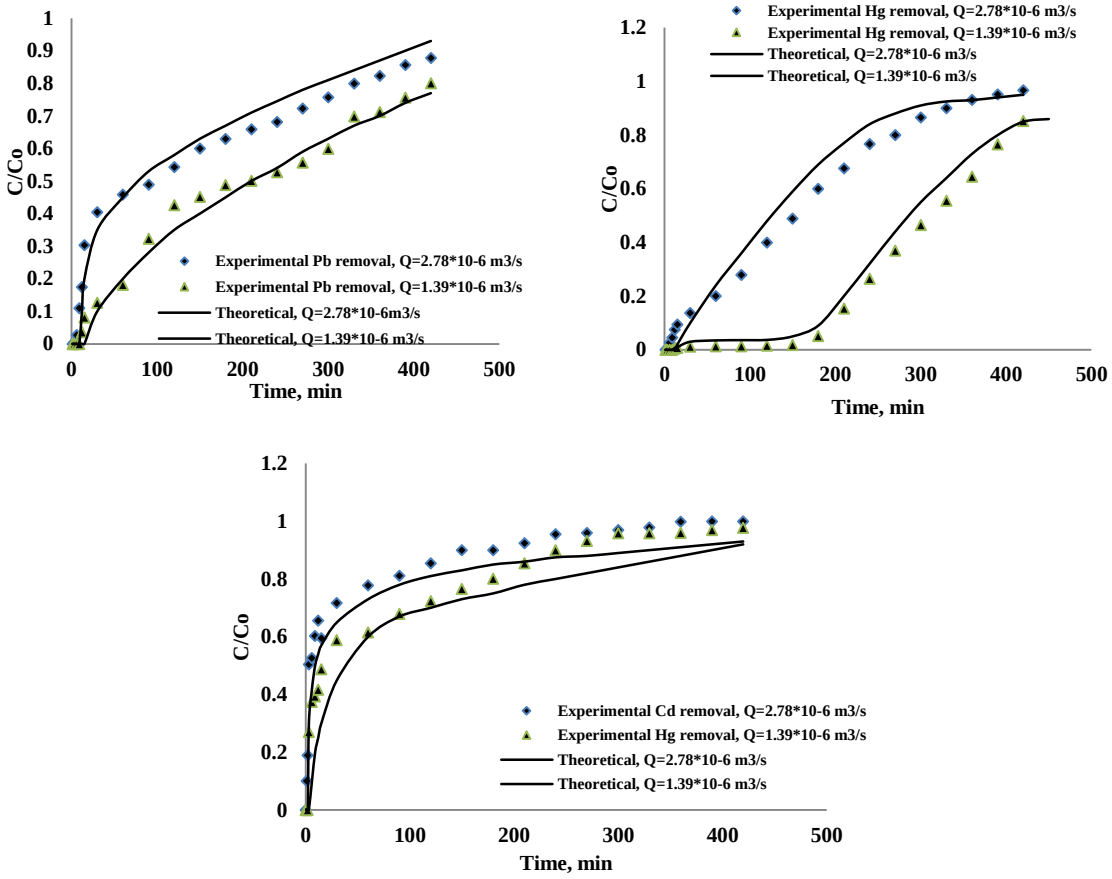

Fig. 12 Experimental and theoretical breakthrough curves for Pb(II), Hg(II), and Cd (II) adsorption onto activated carbon at different flow rates, Co=50 ppm, L=0.1 m (with 5% glass beads bed), and pH=4 for Pb(II) and Hg(II), pH=6 for Cd(II)

ISSN: 2277-9655
Scientific Journal Impact Factor: 3.449
(ISRA), Impact Factor: 1.852

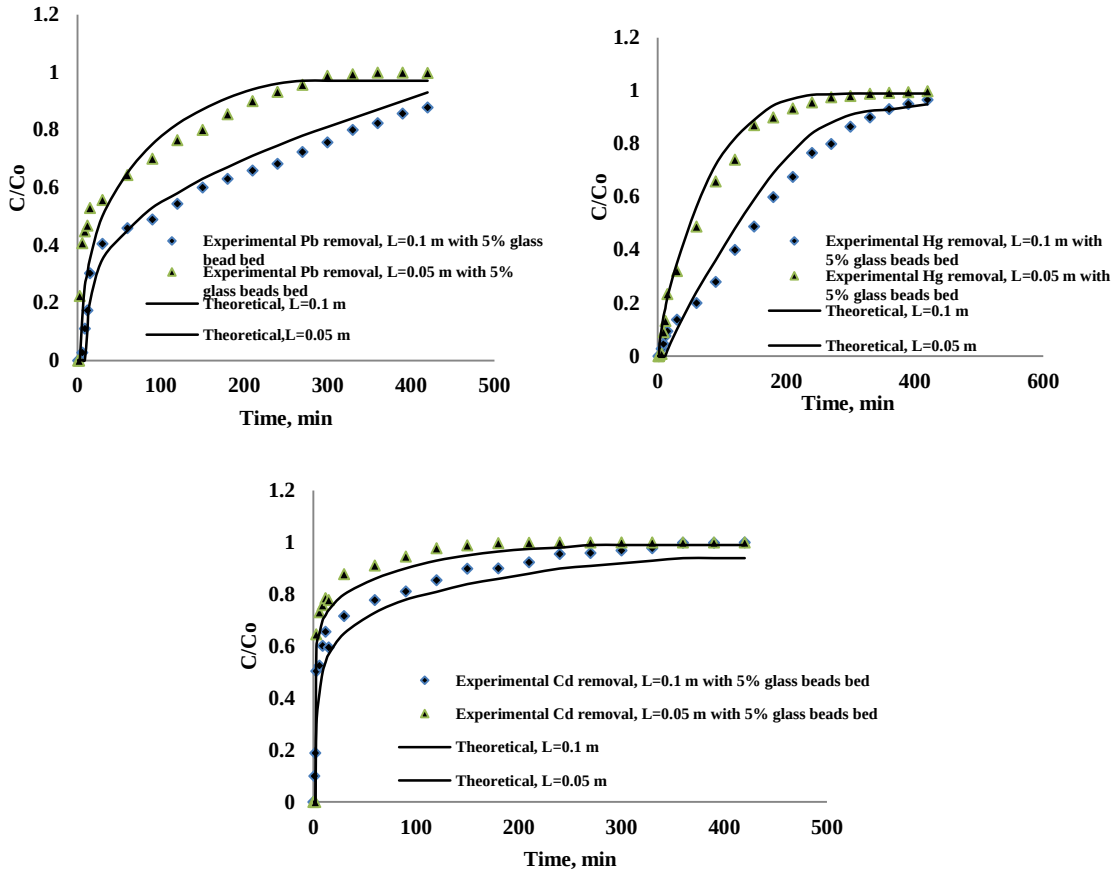

Fig.13 Experimental and theoretical breakthrough curves for Pb(II), Hg(II), and Cd (II) adsorption onto activated carbon at different bed depth (with 5% glass beads bed), Q=2.78×10-6m3/s, Co=50 ppm, and pH=4 for Pb(II) and Hg(II), pH=6 for Cd(II)

ISSN: 2277-9655
Scientific Journal Impact Factor: 3.449
(ISRA), Impact Factor: 1.852

Table 1 Parameters of solute isotherm for Pb (II), Hg (III) and Cd (II) ions onto GAC

Model		Parameters	Pb(II)	Hg(II)	Cd(II)
Freundlich[10]	$q_e = K_F C_e^{1/n}$	K,	3.388	2.855	0.617
		n,-	1.669	2.233	1.815
		R^2	**0.975**	**0.672**	**0.687**
Langmuir [9]	$q_e = \frac{q_m b C_e}{(1 + bC_e)}$	q_m(mg g^{-1})	43.208	16.953	7.5015
		b(L mg^{-1})	0.0478	0.115	0.0393
		R_L	0.01998	0.01995	0.01998
		R^2	**0.9816**	**0.822**	**0.810**
Redlich–Peterson [17]	$q_e = \frac{K_{RP} C_e}{1 + a_{RP} C_e^{\beta_{RP}}}$	k_{RP}(mg g^{-1})	1.768E10	1.319	0.1
		a_{RB}(L mg^{-1})	4.753E8	0.00044	0.247
		ß,-	0.429	2.505	0.0001
		R^2	**0.975**	**0.809**	**0.663**
Sips [10]	$q_e = \frac{K_s C_e^{\beta_s}}{1 + a_s C_e^{\beta_s}}$	k_s	1.908	0.1056	0.647
		ß$_s$	1.051	2.747	0.426
		a_s	0.047	0.0078	0.768
		R^2	**0.981**	**0.768**	**0.688**
Khan [10]	$q_e = \frac{q_m b_k C_e}{(1 + b_k C_e)^{a_k}}$	q_m (mg g^{-1})	184.39	3204	0.195
		b_k,(L mg^{-1})	0.01	0.0005	8.68
		ak	3.007	88.53	0.455
		R2	**0.972**	**0.711**	**0.638**